NUMERICAL STUDY OF FLATNESS BASED MOTION PLANNING FOR A HORIZONTALLY MOVING BEAM WITH A POINT MASS

M. Bachmayer [1], B. Berger[1], J. Rudolph[2], H. Ulbrich [1]
[1] Technische Universität München, Germany, [2]Technische Universität Dresden, Germany

Corresponding author: M. Bachmayer, Technische Universität München, Lehrstuhl für Angewandte Mechanik, 85748 Garching bei München, Boltzmannstraße 15, Germany, *bachmayer@amm.mw.tum.de*

Abstract. Flexibilities of a machine's structure have to be taken into account if high precision and high speed positioning are desired. Thus, the system's efficiency can be increased by consideration of its flexibilities in the control design instead of using a stiffer and, therefore heavier structure. For linearly actuated robots, like placement machines or rack feeders, an explicitly parametrized feed forward control law is presented. Positioning of elastic structures with a constant mass distribution can be performed, by avoiding residual vibrations using a flatness based control law. The efficiency and aspects of robustness of this approach are investigated numerically using a finite element and a finite difference model.

1 Introduction

For systems with a flat output it is simple to calculate feedforward control trajectories. For linear distributed parameter systems a well developed flatness based theory can be found in [2, 3, 4, 6]. Based on this theoretical background a flatness based planning approach based on a very simple mechanical model for a real world mechanism can be found in [1]. Here the simple — yet already very useful — mechanical model used in [1] is further developed into a more detailed mechanical model for unilaterally actuated linear manipulators with a perpendicularly mounted arm subject to vibrations. In view of parametric uncertainties occuring in practice robustness and efficiency of this approach are numerically studied.

2 Moving beam with point mass

In Figure 1 the mechanical model considere is sketched. The vertical structure is modelled by an Euler Bernoulli

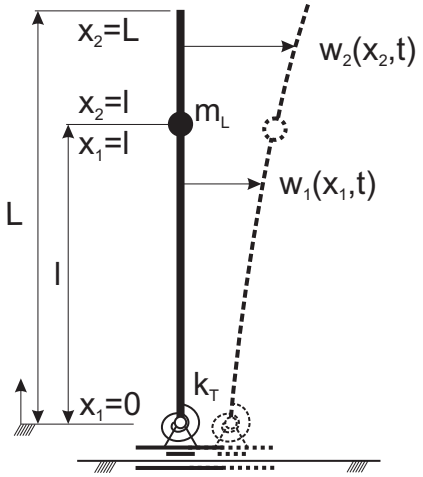

Figure 1: Linear actuator with attached elastic structure. Elasticities of the slide bar are modeled by a rotational stiffness k_T. The structure between the actuator and the payload m_L — for instance a tool like a gripper — as also the structure beyond the mass m_L are taken into account as two Euler-Bernoulli beams.

beam separated into two sections below and above the payload m_L situated at a distance l from the base point. The stiffness of the slide bar is modeled as a rotational spring situated at the base point. This leads to a boundary value problem with eight boundary conditions.

The independent variables, i.e., the positions x_1 and x_2 along the beam segments as well as the time t, are normalized for the calculation:

$$\underline{x}_1 = \frac{x_1}{L}, \qquad \underline{x}_2 = \frac{x_2}{L}, \qquad \underline{t} = \frac{1}{L^2}\frac{\sqrt{EI}}{\sqrt{\rho A}}t, \qquad \underline{l} = \frac{l}{L}. \tag{1}$$

The (normalized) partial differential equations can then be written as

$$\partial^4_{\underline{x}_1} w_1(\underline{x}_1,\underline{t}) + \ddot{w}_1(\underline{x}_1,\underline{t}) = 0 \tag{2}$$

$$\partial^4_{\underline{x}_2} w_2(\underline{x}_2,\underline{t}) + \ddot{w}_2(\underline{x}_2,\underline{t}) = 0. \tag{3}$$

Here $\partial^4_{\underline{x}_i} w_i$ is used to denote the partial derivative $\frac{\partial^4 w_i}{\partial \underline{x}_i^4}$ while $\ddot{w}_i$ denotes $\frac{\partial^2 w_i}{\partial \underline{t}^2}$, $i = 1,2$. The (normalized) boundary conditions read as follows:

$$\alpha\, \partial^2_{\underline{x}_1} w_1(0,\underline{t}) = \partial_{\underline{x}_1} w_1(0,\underline{t}) \tag{4}$$
$$\partial^3_{\underline{x}_1} w_1(0,\underline{t}) = \tilde{u}(\underline{t}) \tag{5}$$
$$w_1(\underline{l},\underline{t}) = w_2(\underline{l},\underline{t}) \tag{6}$$
$$\partial_{\underline{x}_1} w_1(\underline{l},\underline{t}) = \partial_{\underline{x}_2} w_2(\underline{l},\underline{t}) \tag{7}$$
$$\partial^2_{\underline{x}_1} w_1(\underline{l},\underline{t}) = \partial^2_{\underline{x}_2} w_2(\underline{l},\underline{t}) \tag{8}$$
$$\partial^3_{\underline{x}_1} w_1(\underline{l},\underline{t}) + \varphi\, \ddot{w}_1(\underline{l},\underline{t}) = \partial^3_{\underline{x}_2} w_2(\underline{l},\underline{t}) \tag{9}$$
$$\partial^2_{\underline{x}_2} w_2(1,\underline{t}) = 0 \tag{10}$$
$$\partial^3_{\underline{x}_2} w_2(1,\underline{t}) = 0. \tag{11}$$

Here α, φ, and $\tilde{u}(\underline{t})$ are defined as

$$\alpha = \frac{EI}{k_T L}, \qquad \varphi = -\frac{m_L}{\rho L A}, \qquad \tilde{u}(\underline{t}) = -\frac{L^3}{EI}\, u(\underline{t}). \tag{12}$$

Table 1: Short description of boundary conditions

Eq-Nr.	Meaning
(4)	Bending moment at base point equals spring torque.
(5)	Shear force at foot is equal to actuator force.
(6)	Beam deflections at the crosspoint are equal.
(7)	Beam inclinations at the crosspoint are equal.
(8)	Bending moments at the crosspoint are equal.
(9)	Shear forces and inertial force due to load m_L are balanced.
(10)	No torque at the free end of the beam.
(11)	No shearing force at the free end of the beam.

3 Flatness based trajectory planning

It is assumed that the mechanism is at the beginning of the motion at rest:

$$w_1(\underline{x}_1,0) = 0, \qquad w_2(\underline{x}_2,0) = 0, \qquad \dot{w}_1(\underline{x}_1,0) = 0, \qquad \dot{w}_2(\underline{x}_2,0) = 0. \tag{13}$$

Thus, the following ordinary differential equations can be derived by replacing the operator s for derivation w.r.t. $\underline{t}$ (by Laplace transform or Mikusiński's operational calculus):

$$\partial^4_{\underline{x}_1} \hat{w}_1(\underline{x}_1) + s^2 \hat{w}_1(\underline{x}_1) = 0 \tag{14}$$
$$\partial^4_{\underline{x}_2} \hat{w}_2(\underline{x}_2) + s^2 \hat{w}_2(\underline{x}_2) = 0. \tag{15}$$

The following ansatz functions are chosen for $\hat{w}_1$ and $\hat{w}_2$:

$$\hat{w}_1(\underline{x}_1) = a C_1(\underline{x}_1) + b C_2(\underline{x}_1) + c S_1(\underline{x}_1) + d S_2(\underline{x}_1) \tag{16}$$
$$\hat{w}_2(\underline{x}_2) = e C^+(\underline{x}_2) + f C^-(\underline{x}_2) + g S^+(\underline{x}_2) + h S^-(\underline{x}_2) \tag{17}$$

with the operational functions C_1, C_2, S_1, and S_2 in (16) defined as

$$C_1(\underline{x}) = \frac{\cosh(\sqrt{js}\underline{x}) + \cos(\sqrt{js}\underline{x})}{2}, \quad C_2(\underline{x}) = \frac{\cosh(\sqrt{js}\underline{x}) - \cos(\sqrt{js}\underline{x})}{2js},$$
$$S_1(\underline{x}) = \frac{\sinh(\sqrt{js}\underline{x}) + \sin(\sqrt{js}\underline{x})}{2\sqrt{js}}, \quad S_2(\underline{x}) = \frac{\sinh(\sqrt{js}\underline{x}) - \sin(\sqrt{js}\underline{x})}{2(js)^{3/2}}.$$

With these C^+, C^-, S^+, and S^- in (17) are defined as

$$C^+(\underline{x}) = \frac{C+\overline{C}}{2} = \frac{\partial S^-}{\partial \underline{x}}, \qquad C^-(\underline{x}) = \frac{C-\overline{C}}{2j} = \frac{\partial S^+}{\partial \underline{x}}, \tag{18}$$
$$S^+(\underline{x}) = \frac{\overline{S}+jS}{2h\sqrt{s}} = -\frac{1}{s}\frac{\partial C^+}{\partial \underline{x}}, \qquad S^-(\underline{x}) = \frac{-\overline{S}+jS}{2h\sqrt{s}} = \frac{1}{s}\frac{\partial C^-}{\partial \underline{x}} \tag{19}$$

with $C(\underline{x}) = \cosh[h\sqrt{s}(1-\underline{x})]$, $S(\underline{x}) = \sinh[h\sqrt{s}(1-\underline{x})]$, $j = \sqrt{-1}$, and $h = \exp(j\pi/4)$. Moreover, $\overline{C}$, $\overline{S}$, and $\overline{h}$ denote the complex conjugates of C, S, and h. Using the ansatz (16)–(17) in the boundary conditions (4), (5), (10), and (11) it follows that $c = \alpha b$, $d = \hat{\tilde{u}}$, $f = 0$, $g = 0$. Thus, (16) and (17) simplify to

$$\hat{w}_1(\underline{x}_1) = a\,C_1(\underline{x}_1) + b\,C_2(\underline{x}_1) + \alpha\,b\,S_1(\underline{x}_1) + \hat{\tilde{u}}\,S_2(\underline{x}_1) \tag{20}$$

$$\hat{w}_2(\underline{x}_2) = e\,C^+(\underline{x}_2) + h\,S^-(\underline{x}_2). \tag{21}$$

Using (20), (21) in the other boundary conditions (6)–(9), an (inhomogeneous) linear system of equations for the four unknown parameters a, b, e, h can be derived:

$$\begin{aligned}
aC_1(\underline{l}) + b[C_2(\underline{l}) + \alpha S_1(\underline{l})] + \hat{\tilde{u}}S_2(\underline{l}) &= eC^+(\underline{l}) + hS^-(\underline{l}) \\
-as^2S_2(\underline{l}) + b\,[S_1(\underline{l}) + \alpha C_1(\underline{l})] + \hat{\tilde{u}}C_2(\underline{l}) &= -seS^+(\underline{l}) + hC^+(\underline{l}) \\
-as^2C_2(\underline{l}) + b[C_1(\underline{l}) - \alpha s^2S_2(\underline{l})] + \hat{\tilde{u}}S_1(\underline{l}) &= -seC^-(\underline{l}) - shS^+(\underline{l}) - as^2S_1(\underline{l}) \\
&\quad + \hat{\tilde{u}}C_1(\underline{l}) - b[s^2S_2(\underline{l}) + \alpha s^2C_2(\underline{l})] \\
\varphi s^2[aC_1(\underline{l}) + b[C_2(\underline{l}) + \alpha S_1(\underline{l})] + \hat{\tilde{u}}S_2(\underline{l})] &= -s^2eS^-(\underline{l}) - shC^-(\underline{l}).
\end{aligned}$$

Replacing these parameters in the solution (20), (21) one obtains a representation of the form

$$Q_1\hat{w}_1(\underline{x}_1) = P_1(\underline{x}_1)\hat{\tilde{u}} \tag{22}$$

$$Q_2\hat{w}_2(\underline{x}_2) = P_2(\underline{x}_2)\hat{\tilde{u}}. \tag{23}$$

After multiplication of (22) with P_2 and (23) with P_1, $\hat{\tilde{u}}$ can be eliminated, thus

$$P_2(\underline{x}_2)Q_1\hat{w}_1(\underline{x}_1) = P_1(\underline{x}_1)Q_2\hat{w}_2(\underline{x}_2). \tag{24}$$

Here a new "free parameter" $\hat{y}_0$ is introduced:

$$\hat{w}_1(\underline{x}_1) = P_1(\underline{x}_1)Q_2\hat{y}_0 \tag{25}$$

$$\hat{w}_2(\underline{x}_2) = P_2(\underline{x}_2)Q_1\hat{y}_0 \tag{26}$$

$$\hat{\tilde{u}} = Q_1Q_2\hat{y}_0. \tag{27}$$

This new variable $\hat{y}_0$ is called a flat output of the system [2, 4]. Use of this flat output would allow a parameterization of the complete system trajectories.

Anyhow, a slight simplification results by parametrizing trajectories of the lower beam only. To this end, one may introduce $\hat{y}$ as

$$\hat{y} = Q_2\hat{y}_0. \tag{28}$$

It is obvious from (25) and (27) that this allows to parameterize trajectories of w_1 and $\tilde{u}$. This is done in the sequel.

By a calculation similar to what is done in [2, 4], viz. a series expansion of the (transcendental) operational functions involved in the expressions of P_1 and Q_1, sorting, interpretation of powers of s as differentiation w.r.t. time, the beam deflection $w_1(\underline{x}_1, \underline{t})$ is obtained as

$$w_1(\underline{x}_1, \underline{t}) = \sum_{n=0}^{\infty}(-1)^n\left(p_{1,n}(\underline{x}_1)\frac{y^{(2n)}(t)}{(4n)!} + p_{2,n}(\underline{x}_1)\frac{y^{(2n+2)}(t)}{(4n+2)!} + p_{3,n}(\underline{x}_1)\frac{y^{(2n+2)}(t)}{(4n+3)!}\right), \tag{29}$$

and the actuator force is

$$u(\underline{t}) = \frac{EI}{L^3}\left(\alpha\frac{y^{(2)}(t)}{2} - \sum_{n=0}^{\infty}(-1)^n\left(q_{1,n}\frac{y^{(2n+2)}(t)}{(4n+1)!} + q_{2,n}\frac{y^{(2n+4)}(t)}{(4n+3)!}\right)\right). \tag{30}$$

Here

$$
\begin{aligned}
p_{1,n}(\underline{x}_1) =& \frac{1}{2}\left(\underline{x}_1^{4n} + (\mathrm{Re}+\mathrm{Im})\{(1-\underline{x}_1+j)^{4n}\}\right),\\
p_{2,n}(\underline{x}_1) =& \frac{\alpha\varphi}{4}(\mathrm{Im}\{(\underline{x}_1-1+j)^{4n+2}\} + \mathrm{Im}\{(\underline{x}_1-\underline{l}+\underline{l}j)^{4n+2}\})\\
&+\frac{\alpha\varphi}{8}\left[(\mathrm{Re}-\mathrm{Im})\{(\underline{l}-1+\underline{x}_1+(\underline{l}-1)j)^{4n+2}\}\right.\\
&-\mathrm{Re}\{(\underline{x}_1-\underline{l}+1-(\underline{l}-1)j)^{4n+2}\}+\mathrm{Im}\{(\underline{x}_1-\underline{l}+1+(\underline{l}-1)j)^{4n+2}\}\left.\right]\\
&+\frac{\alpha\varphi}{8}\left[(\mathrm{Re}-\mathrm{Im})\{(\underline{x}_1-1-(2\underline{l}-1)j)^{4n+2}\}\right.\\
&-(\mathrm{Re}-\mathrm{Im})\{(\underline{x}_1-2\underline{l}+1+j)^{4n+2}\}\left.\right],\\
p_{3,n}(\underline{x}_1) =& -\frac{\alpha}{2}x^{4n+3} + (\frac{\alpha}{2}-\frac{\varphi}{4})\,\mathrm{Re}\{(x-1-j)^{4n+3}\} - \frac{\alpha}{2}\,\mathrm{Im}\{(x-1-j)^{4n+3}\}\\
&+\frac{\varphi}{2}\,\mathrm{Re}\{(\underline{l}-x+\underline{l}j)^{4n+3}\}+\frac{\varphi}{8}\left[(\mathrm{Re}-\mathrm{Im})\{(\underline{l}-1+x+(\underline{l}-1)j)^{4n+3}\}\right.\\
&+(\mathrm{Re}-\mathrm{Im})\{(\underline{l}-1-x+(\underline{l}-1)j)^{4n+3}\}\left.\right]\\
&-\frac{\varphi}{8}\left[(\mathrm{Re}-\mathrm{Im})\{(x-2\underline{l}+1-j)^{4n+3}\}\right. +(\mathrm{Re}-\mathrm{Im})\{(x-1+(2\underline{l}-1)j)^{4n+3}\}\left.\right],\\
q_{1,n} =& [(-4)^n\left(\frac{\alpha}{2}-\frac{\varphi}{4}-\underline{l}\frac{\varphi}{2}\right)+(2\underline{l}-1+j)^{4n}\,\frac{\varphi}{8}\,(-1-j)+\\
&+(2\underline{l}-1-j)^{4n}\,\frac{\varphi}{8}\,(j-1)]\,(4n+1)+(-4)^n,\\
q_{2,n} =& \left\{(-4)^{n+1}\,(1+2\underline{l}^{4n+3}-2(\underline{l}-1)^{4n+3})+2\,\mathrm{Re}\{(1+(2\underline{l}-1)j)^{4n+3}\}\right\}\frac{\varphi\alpha}{8}.
\end{aligned}
$$

4 Parametrization of the flat output trajectory

In order to satisfy the homogeneous initial conditions and in order to guarantee series convergence trajectories $t \mapsto y(t)$ are chosen in such a way that the following conditions are met [2, 4]:

- $y : \mathbf{R} \to \mathbf{R}$ is a $\mathscr{C}^\infty$ function,
- $y(t) = 0$ for $t \le 0$,
- $y(t) = y_T^*$ for $t \ge t_*$,
- y is a Gevrey function of class $\alpha < 2$.

This means that $y^{(i)}(0) = 0$ for $i \le 0$ and $y^{(i)}(t_*) = 0$ for $i > 0$ is accomplished. Thus, the function must be smooth and cannot be an analytical function unless it is identical to zero.

An appropriate choice for such trajectories is

$$t \mapsto y^*(t) = y_T^*\,\Theta(t) \tag{31}$$

where y_T^* defines the final position at which the device should be positioned. Furthermore, Θ is defined by

$$\Theta(t) = \begin{cases} 0 & t \le 0 \\ \frac{\int_0^t \Theta_{\sigma,T}(\tau)d\tau}{\int_0^T \Theta_{\sigma,T}(\tau)d\tau} & t \in (0,T) \\ 1 & t \ge 0 \end{cases} \tag{32}$$

and $\Theta_{\sigma,T}(t) = \exp\left(-1/\left[\left(1-\frac{t}{T}\right)\frac{t}{T}\right]^\sigma\right)$ on the interval $(0,T)$ and vanishes outside.

5 Planning results

The following planning results for a highly dynamic positioning of the device can be achieved with the analytical planning algorithm proposed. The field of deflection over the time t is plotted in Figure 2, while snapshots of the system during a planned motion are shown in Figure 3.

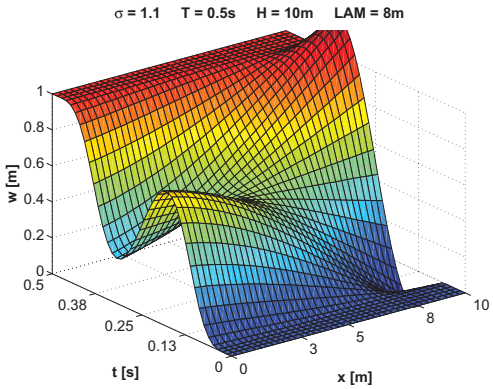

Figure 2: Field of beam deflection over time

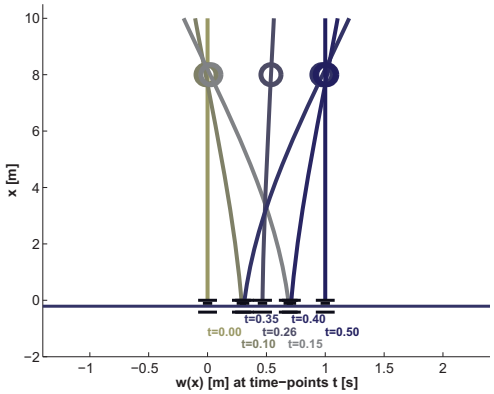

Figure 3: Phases of positioning movement

6 Simulation results

6.1 Using a FEM model

A simulation result performed with the multi body simulation program MBSIM[1] is shown in Figure 4. Here a device with a pylon height of 10 m is simulated. Positioning of the device over 1.15 m with about 800 kg overall mass is performed in 1 s. This yields a manoeuvre with force amplitudes according to the available maximum of a real world device. The total payload m_L is 180 kg, where 80 kg are the mass of the tool itself. Residual vibrations have an amplitude of about 1 mm. The load is in a height of 9 m.

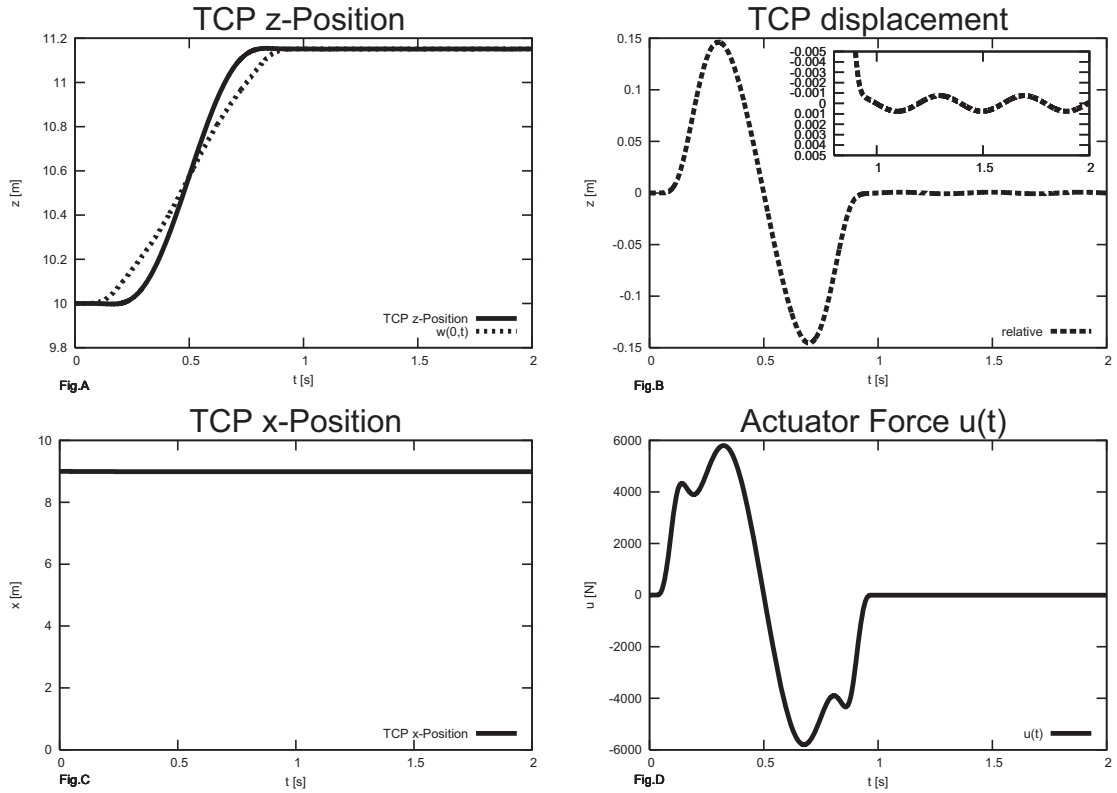

Figure 4: Simulation results: Fig A: movement of Tool Center Point (TCP), Fig B: difference between TCP- and foot-z position, Fig C: x-position of payload, Fig D :actuator force

[1] Multi-Body Simulation software: http://mbsim.berlios.de

6.2 Using a finite difference model

For a controller design — e.g., a state feedback controller - a discrete model of the system dynamics is desirable. A model based on finite differences is presented here. The mechanical model is shown in Figure 5. Note that here torques of inertia caused by the payload are neglected. For systems consisting of two pylons there are indeed no such torques, because of the parallel kinematics. For systems consisting of a single beam, it has to be verified, whether the assumption that the payload's torques of inertia have negligible effect on the beam's dynamic. The Euler Bernoulli Beam is modeled by finite differences (Figure 6), the payload m_L is attached to the beam through a horizontally translational stiffness c_{TCP}.

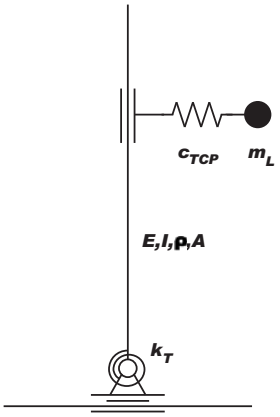

Figure 5: Mechanical model

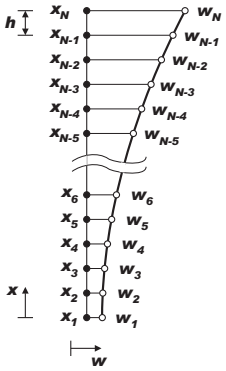

Figure 6: Discrete model

Because this discrete model is much faster than the high level fem model, it will be used further on for investigations about the robustness of the planning approach. In Figures 7, 8 and 9 the residual vibrations are plotted as a function of nodes and the stiffness c_{TCP}. For a high spring stiffness the magnitude of residual vibrations is a measure for the error introduced by the discretization. For the further investigations, twenty nodes will be used.

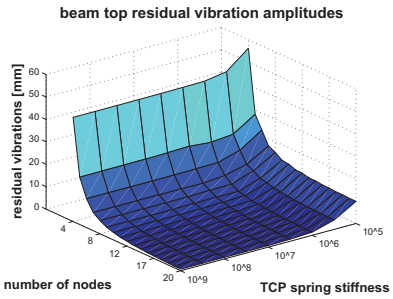

Figure 7: Amplitudes at the top of the beam

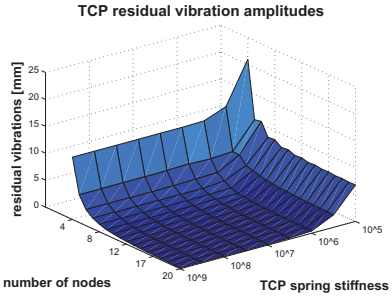

Figure 8: Amplitudes at the Tool Center Point (TCP)

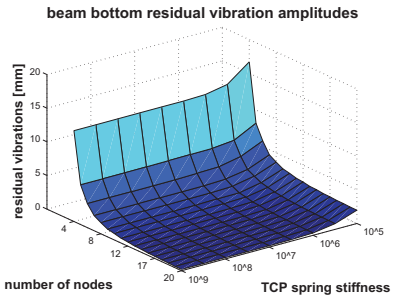

Figure 9: Vibration amplitudes at the bottom of the device

7 Investigation of robustness

The robustness of the presented planning approach is numerically investigated. Two different actuator forces generated by flatness based trajectory planning are considered — for 1 second and 2 second transition time — shown in Figure 10. The effects of parameter deviations on the occurring residual vibrations are investigated by systematic parameter variation and numerical simulation. In Figure 11 and 12 simulation results for various TCP heights are plotted. As expected, the height of the mass is a very sensible parameter. For instance, with a real world TCP height of 7 m residual vibrations have got an amplitude of more than 10 mm.
In Figure 13 the amplitudes of residual vibrations are given for different TCP heights and several transition times. It is obvious that the robustness increases with longer transistion times. In Figure 14 the payload m_L is varied and Figure 15 shows a Variation of the beam length.
In Figure 16 the robustness for the bending stiffness EI, in Figure 17 the robustness for the beam mass ρA, and in Figure 18 the robustness for the rotational stiffness k_T are shown. Thus, it appears that big amplitudes of residual vibrations (>10mm) must only be expected for big differences of parameters (>15%) and short transition times (<2s).

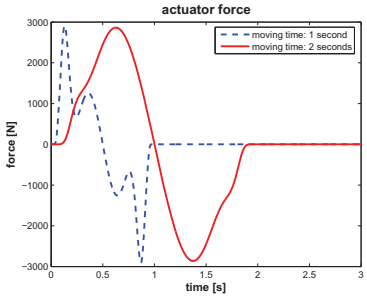

Figure 10: Actuator force trajectories for two transition times

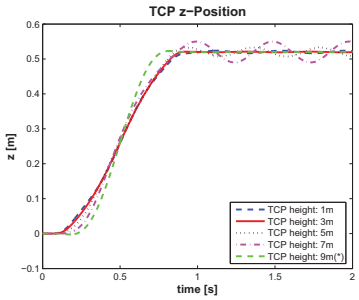

Figure 11: Horizontal TCP trajectories for different TCP heights, for a transition time of 1 second

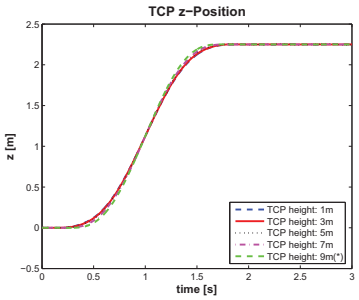

Figure 12: Horizontal TCP trajectories for different TCP heights, for a transistion time of 2 seconds

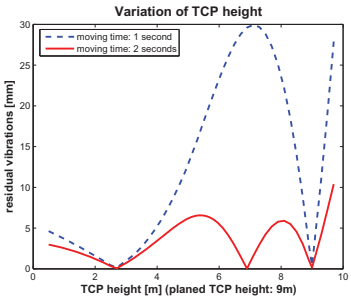

Figure 13: Variation of the TCP height

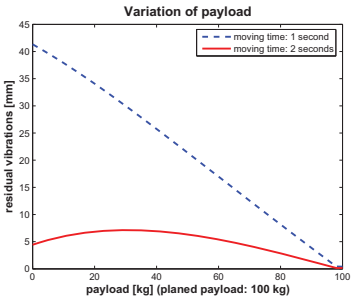

Figure 14: Variation of the payload from 0 kg up to 100 kg

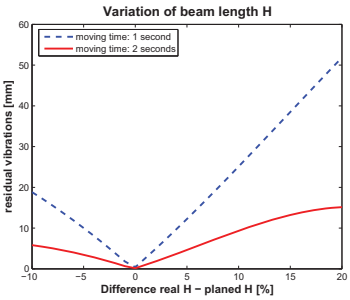

Figure 15: Variation of the beam length

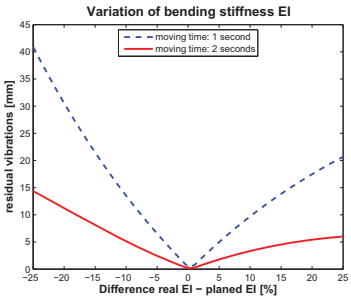

Figure 16: Variation of the bending stiffness EI

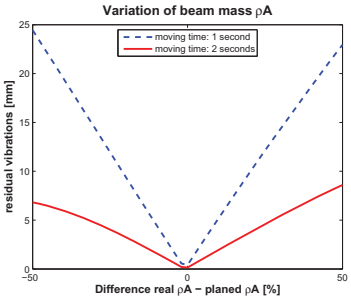

Figure 17: Variation of the beam mass ρA

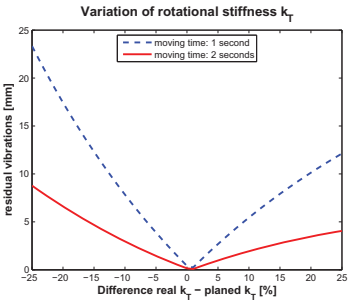

Figure 18: Variation of the rotational stiffness k_T

8 Conclusion

Using the here presented flatness based planning approach positioning with very low residual vibrations can be performed. Robustness against variations of the payload and its height has been studied numerically. Compared to standard trajectories of today's drives the results are very good even with large parameter variations. For faster trajectories the robustness decreases. Therefore, this planning approach may be considered as rather robust. For heights larger than 10 m this enhanced approach shows better characteristics than the simple approach presented in [1].

9 References

[1] Bachmayer, M., Ulbrich, H.: Trajectory planning for linearly actuated elastic robots using flatness based control theory. International Conference of Theoretical and Applied Mechanics 2008; Adelaide (August 2008).

[2] Rudolph, J.: Flatness Based Control of Distributed Parameter Systems. Shaker Verlag, Aachen (2003).

[3] Rudolph, J., Woittennek, F.: Flachheitsbasierte Steuerung eines Timoshenko-Balkens. ZAMM **83**, 119–127 (2003).

[4] Rudolph, J.: Beiträge zur flachheitsbasierten Folgeregelung linearer und nichtlinearer Systeme endlicher und unendlicher Dimension. Shaker Verlag, Aachen (2003).

[5] Aoustin, Y., Fliess, M., Mounier, H., Rouchon, P., Rudolph, J.: Theory and practice in the motion planning and control of a flexible robot arm using Mikusinski operators. In: Proc. 5th Symposium on Robotics and Control, Nantes, France, 287–293 (1997).

[6] Woittennek, F.: Beiträge zum Steuerungsentwurf für lineare, örtlich verteilte Systeme mit konzentrierten

Stelleingriffen. Shaker Verlag, Aachen (2007).
[7] Breitenecker, F. and Solar D.: *Models, Methods, Experiments – Modern aspects of simulation languages*. In: Proc. 2nd European Simulation Conference, Antwerpen, 1986, SCS, San Diego, 1986, 195–199.
[8] Casti, J. L.: *Reality Rules – Picturing the World in Mathematics: I, II*. Wiley, New York, 1992.
[9] Sage, A. P.: *Dynamic Systems*. In: Concise Encyclopedia of Modelling and Simulation, (Eds.: Atherton, D. and Borne P.), Pergamon, Oxford, 1992, 91–92.
[10] Troch, I.: *Modelling for optimal control of systems*. Surveys on Mathematics for Industry, 5 (1995), 203–292.